

AD-A157 655

AN ALTERNATIVE INTERPRETATION OF ION RING DISTRIBUTION
OBSERVED BY THE S3. (U) AEROSPACE CORP EL SEGUNDO CA
SPACE SCIENCES LAB D J GORNEY 15 MAY 85

1/1

UNCLASSIFIED

TR-0084R(S940-05)-3 SD-TR-85-14

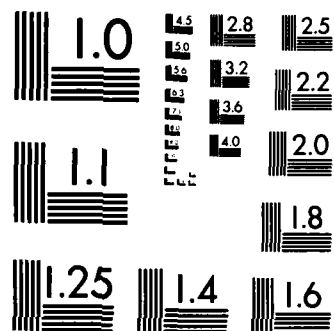
F/G 4/1

NL

END

FILED

DEC



MICROCOPY RESOLUTION TEST CHART
NATIONAL BUREAU OF STANDARDS-1963-A

AD-A157 655

An Alternative Interpretation of Ion Ring Distribution Observed by the S3-3 Satellite

D. J. GORNEY
Space Sciences Laboratory
Laboratory Operations
The Aerospace Corporation
El Segundo, CA 90245

15 May 1985

APPROVED FOR PUBLIC RELEASE;
DISTRIBUTION UNLIMITED

DTIC FILE COPY

Prepared for
SPACE DIVISION
AIR FORCE SYSTEMS COMMAND
Los Angeles Air Force Station
P.O. Box 92960, Worldway Postal Center
Los Angeles, CA 90009-2960




85 7 23 048

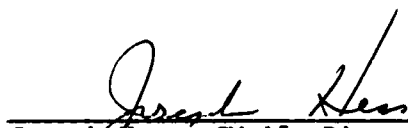
This report was submitted by The Aerospace Corporation, El Segundo, CA 90245, under Contract No. F04701-83-C-0084 with the Space Division, P.O. Box 92960, Worldway Postal Center, Los Angeles, CA 90009-2960. It was reviewed and approved for The Aerospace Corporation by H. R. Rugge, Director, Space Sciences Laboratory. First Lieutenant Douglas R. Case, SD/YCC, was the project officer for the Mission-Oriented Investigation and Experimentation (MOIE) program.

This report has been reviewed by the Public Affairs Office (PAS) and is releasable to the National Technical Information Service (NTIS). At NTIS, it will be available to the general public, including foreign nationals.

This technical report has been reviewed and is approved for publication. Publication of this report does not constitute Air Force approval of the report's findings or conclusions. It is published only for the exchange and stimulation of ideas.



Douglas R. Case, 1st Lt, USAF
Project Officer



Joseph Hess, GM-15, Director, West
Coast Office, AF Space Technology
Center

UNCLASSIFIED

SECURITY CLASSIFICATION OF THIS PAGE (When Data Entered)

REPORT DOCUMENTATION PAGE		READ INSTRUCTIONS BEFORE COMPLETING FORM
1. REPORT NUMBER SD-TR-85-14	2. GOVT ACCESSION NO. D-41576.53	3. RECIPIENT'S CATALOG NUMBER
4. TITLE (and Subtitle) AN ALTERNATIVE INTERPRETATION OF ION RING DISTRIBUTION OBSERVED BY THE S3-3 SATELLITE		5. TYPE OF REPORT & PERIOD COVERED
7. AUTHOR(s) D. J. Gorney		6. PERFORMING ORG. REPORT NUMBER TR-0084A(5940-05)-3
9. PERFORMING ORGANIZATION NAME AND ADDRESS The Aerospace Corporation El Segundo, CA 90245		8. CONTRACT OR GRANT NUMBER(s) F04701-83-C-0084
11. CONTROLLING OFFICE NAME AND ADDRESS Space Division Los Angeles Air Force Station Los Angeles, CA 90009-2960		10. PROGRAM ELEMENT, PROJECT, TASK AREA & WORK UNIT NUMBERS
14. MONITORING AGENCY NAME & ADDRESS (if different from Controlling Office)		12. REPORT DATE 15 May 1985
		13. NUMBER OF PAGES 13
		15. SECURITY CLASS. (of this report) Unclassified
		15a. DECLASSIFICATION/DOWNGRADING SCHEDULE
16. DISTRIBUTION STATEMENT (of this Report) Approved for public release; distribution unlimited.		
17. DISTRIBUTION STATEMENT (of the abstract entered in Block 20, if different from Report)		
18. SUPPLEMENTARY NOTES		
19. KEY WORDS (Continue on reverse side if necessary and identify by block number) Ions Plasma waves		
20. ABSTRACT (Continue on reverse side if necessary and identify by block number) Recently, theoretical interest has grown in possible plasma wave instabilities arising from free energy in auroral ion distributions, and a number of ion-mode instabilities have been identified. These instabilities typically rely on positive slopes in the ion's velocity distribution parallel ($\partial f / \partial v > 0$) or perpendicular ($\partial f / \partial v_\perp > 0$) to the magnetic field. Upflowing ion beams generated by electrical potential drops along auroral field lines are obvious candidates for the parallel (beam) instability, while ion conics have been treated in the limit of the flute mode instability,		

DD FORM 1473
(FACSIMILE)

UNCLASSIFIED

SECURITY CLASSIFICATION OF THIS PAGE (When Data Entered)

UNCLASSIFIED

SECURITY CLASSIFICATION OF THIS PAGE(When Data Entered)

19. KEY WORDS (Continued)

20. ABSTRACT (Continued)

assuming that a positive perpendicular gradient exists. However, ion conics are not responsible for the condition $\partial f / \partial v_{\perp} > 0$. Downflowing ion beam distributions can have $\partial f / \partial v_{\perp} > 0$ and therefore might lead to flute mode instability. Examples of both conics and downflowing beams are presented, showing that only the downflowing component leads to significant $\partial f / \partial v_{\perp} > 0$, while ion conics generally have $\partial f / \partial v_{\perp} < 0$ and are themselves stable to the flute mode.

UNCLASSIFIED

SECURITY CLASSIFICATION OF THIS PAGE(When Data Entered)

CONTENTS

I.	INTRODUCTION.....	5
II.	DATA.....	9
III.	CONCLUSIONS.....	15
	REFERENCES.....	17



Accession For

THIS GRANT

THIS TAB

RESEARCH

1955-1956

FIGURES

1. An energetic ion velocity-space distribution from
S3-3 on 18 July 1976 at 1:08:15 U.T..... 7
2. Two plots of ion density as a function of
velocity for the data shown in Figure 1..... 11
3. Ion distributions from the S3-3 satellite at
high latitude, near apogee on the dayside, showing
a downflowing ion distribution with a peak near
400 km/sec, and an ion conic distribution with no
downflowing ion beam..... 12

I. INTRODUCTION

Observations of approximately kiloelectronvolt auroral ions flowing parallel to the magnetic field have been reported by a number of experimenters (see Shelley et al., 1976 a and b; Sharp et al., 1977; Ghielmetti et al., 1978, 1979; Gorney et al., 1981). Ion distributions with strong perpendicular anisotropies (ion conics) suggestive of cyclotron heating are also common (Sharp et al., 1977; Klumpar, 1979; Gorney et al., 1981; Kintner and Gorney, 1982). Recent theoretical interest in possible instabilities arising from free energy in these auroral ion distributions (e.g., Kintner, 1980; Cattell and Hudson, 1982; Roth and Hudson, 1982; Kaufman and Kintner, 1982) has required numerical modeling of the ion distributions, and a number of ion-mode instabilities have been identified.

Upflowing ion beams are generally considered to be the result of acceleration of ionospheric ions by electrical potential drops along the auroral field lines, and typically have been modeled as a hot ion population drifting upward with respect to cold background ions and electrons (e.g., Kaufman and Kintner, 1982).

Downflowing ion beams are quite rare compared to upflowing beams (Ghielmetti et al., 1979), but downflowing ions in the low-altitude cusp region are quite common, and can have beam-like distributions (Shelley et al., 1976 a and b; Reiff et al., 1977; Burch et al., 1982). The magnetic defocusing of these downstreaming distributions can lead to the formation of rings of ions in perpendicular velocity as well as positive gradients in parallel velocity.

Ion conics are upflowing ion distributions with strong perpendicular anisotropies. Conics are thought to be formed by perpendicular heating at low altitudes by EIC or VLF waves (Ungstrup et al., 1979; Lysak et al., 1980; Chang and Coppi, 1981; Dusenbery and Lyons, 1981; Okuda and Abdalla, 1981) or perhaps by stochastic energization by small-scale electrostatic fields (Lennartsson, 1980; Greenspan and Whipple, 1982). Ion conics are observed at all local times in the auroral latitudes, and are thought to be generated near

or below 2000 km altitude (Klumpar, 1979; Gorney et al., 1981). Conics typically have power-law energy spectra over the energy range from 10 eV to 4 keV (Fennell et al., 1979; Klumpar, 1979). Since conics are generated above the atmosphere, their angular distributions contain an atmospheric loss cone. At altitudes much higher than 2000 km, ion conics have relative flux maxima at pitch angles between 90° and 180° (i.e., a conical distribution) due to the magnetic focussing of an original pancake distribution. Simultaneous observations of upflowing ion conics and downstream cusp ions are common on the dayside, although few of these observations have been reported in the literature. An example of such an event is presented in Figures 1 and 2 of Cattell and Hudson (1982).

An ion distribution from the period discussed by Cattell and Hudson is presented in Figure 1 of this report. This ion distribution is coincident with wave emissions near the lower hybrid resonance frequency, which can be described in terms of a flute mode instability. Cattell and Hudson argued that the ion conic population is responsible for the observed positive velocity gradient in the ion distribution that is necessary for instability. Examination of these data shows that the ion conic does not contribute a positive perpendicular velocity gradient to the ion distribution, but that two regions of positive perpendicular velocity gradient do exist in the observed distribution, because of the atmospheric loss cone at high energy and the downstream energetic ions. Two other data examples are presented in this report, showing a downstream ion event and an ion conic event separately. The downstream ion event shows a ring of ions even in the absence of an ion conic. The ion conic example shows no positive velocity gradients other than the high-energy loss cone.

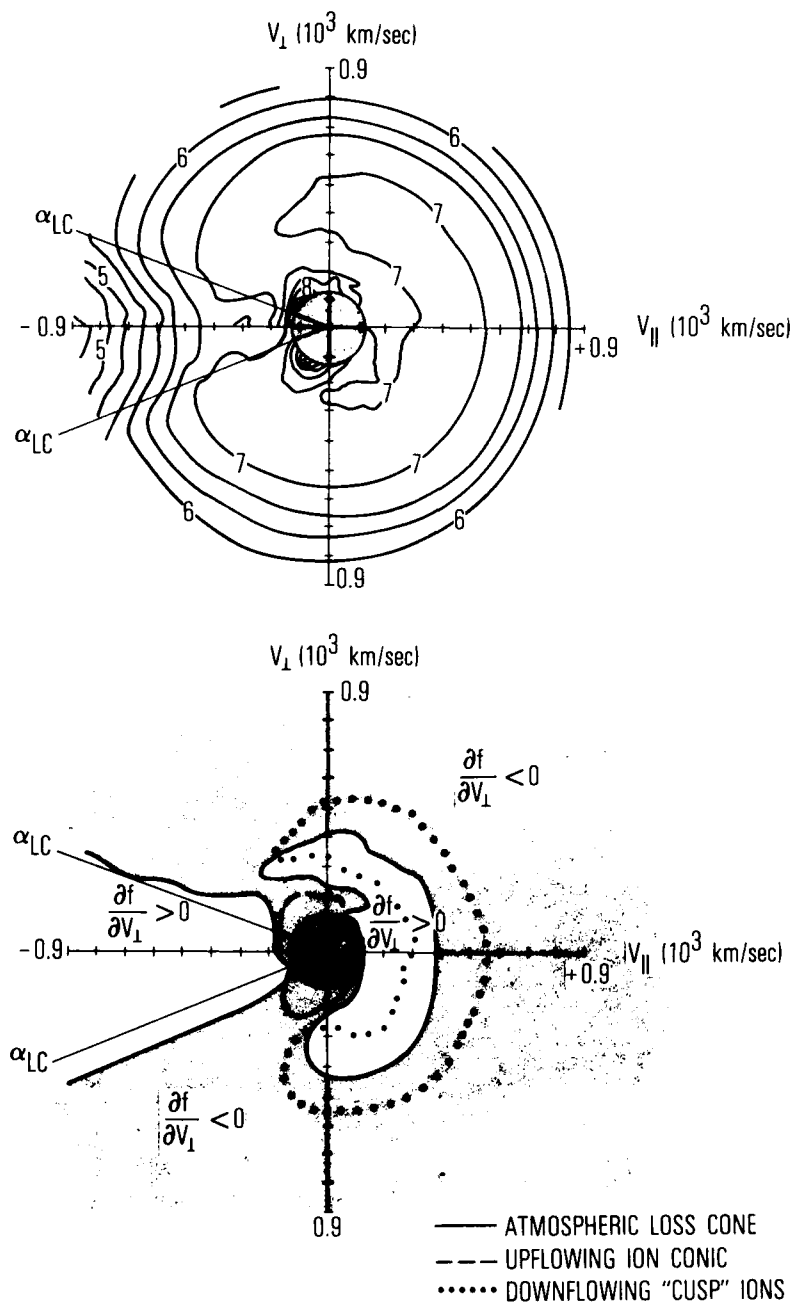


Fig. 1. An energetic ion velocity-space distribution from S3-3 on 18 July 1976 at 1:08:15 U.T. The $+v_{\parallel}$ direction corresponds to downflowing ions. The computed loss cone is labeled α_{LC} . The lower panel indicates regions of positive (unshaded) and negative (shaded) perpendicular gradient $\partial f / \partial v_{\perp}$. The atmospheric loss cone, ion conic, and downflowing ion beam are outlined.

II. DATA

The upper panel of Figure 1 shows a contour plot of the energetic ion velocity space distribution observed by the S3-3 satellite at 01:08:15 U.T. (± 10 sec) on 18 July 1976. In this plot the $+v_{\parallel}$ axis corresponds to downflowing particles. The distribution function contours are logarithmic (the contour labeled 7 corresponds to a distribution function value of 10^7 sec^3/km^6). At this time S3-3 was near 7800 km altitude, and at 10.7 hr local time.

Several interesting features are apparent in this ion distribution, which is characteristic of the ion distributions observed throughout the 1-min period of interest. First, the atmospheric loss cone is apparent at upflowing velocities greater than 200 km/sec. The computed extent of the 100 km loss cone is labeled α_{LC} on the figure. The tightly packed contours at velocities less than 250 km/sec in the upflowing hemisphere represent the typical signature of an ion conic. The ion conic extends to energies of about 290 eV, and no ion conic exceeds 470 eV in the entire period in which wave emissions were observed. This conic has a relative flux maximum at a pitch angle of about 125° . The remainder of the ion distribution is isotropic in pitch angle, but with a ring of ions in the downflowing hemisphere.

This ion ring is outlined by the contour labeled 7, and close inspection of the density distribution either in the downflowing or perpendicular direction reveals a relative minimum at about 250 km/sec and a relative maximum at about 400 km/sec.

Perpendicular velocity gradients were computed for these data, and the boundaries between regions of $\partial f / \partial v_{\perp} > 0$ and $\partial f / \partial v_{\perp} < 0$ are shown in the lower panel of Figure 1. The shaded region corresponds to $\partial f / \partial v_{\perp} < 0$; the unshaded regions have the positive gradients required for instability. The atmospheric loss cone, the ion conic, and the downflowing beam regions are outlined with a thin solid line, a thin dashed line, and a dotted line respectively. As expected, the loss cone is a region of $\partial f / \partial v_{\perp} > 0$, whereas the ion conic has $\partial f / \partial v_{\perp} < 0$. The low-velocity edge of the downflowing ion beam, extending to

90° pitch angle, is a region of positive perpendicular gradient. It is important to note that the unshaded regions represent the only regions that can contribute to the flute mode instability.

Cattell and Hudson, describing the quantity $\int f(v_{\parallel}, v_{\perp}) dv_{\parallel}$ for a time period surrounding 1:08:26 U.T., noted a region of positive slope between 200 and 300 km/sec perpendicular velocity, which they attributed to the presence of the ion conic. It is clear from the bottom panel of Figure 1 that the observed positive slope must be due to the downflowing ion beam, and not the upflowing ion conic. This point is seen even more clearly in Figure 2, which directly compares the roles of the downflowing beam and upflowing ion conic in producing a positive slope in perpendicular velocity. (Note that data from the period surrounding 1:08:15 are plotted in these figures. This period was chosen for study because the data are more time stationary than at 1:08:26 and well within the interval when the waves were observed.)

The two panels of Figure 2 show ion distributions for the same data presented in Figure 1. The left panel compares the upflowing ion velocity distribution (dashed line) with that at 90° pitch angle (solid line); the right panel compares the 0° pitch angle (dashed line) with the perpendicular flux (solid line). The broad arrow in the left panel indicates the highest velocity at which conical ion distributions were observed. The perpendicular ion distribution function has a peak near 400 km/sec and a positive slope between 200 and 300 km/sec. The same spectral shape is also apparent in the downflowing population in the right panel. The ion conic has a steep, monotonically decreasing spectrum over the entire energy range in which it maintains a conical pitch angle distribution. Clearly, the perpendicular spectrum is due to the magnetic defocussing of the downflowing ion distribution, and the ion conic can only decrease the positive gradient between 200 and 400 km/sec.

Figure 3 shows independent examples of downflowing ions (a) and an upflowing ion conic (b). Both examples are from S3-3 near apogee, at high latitude on the dayside. The downflowing ions have a peak near 400 km/sec,

S3-3 REV. 73 1:08:04 U.T. 18 JULY 1976

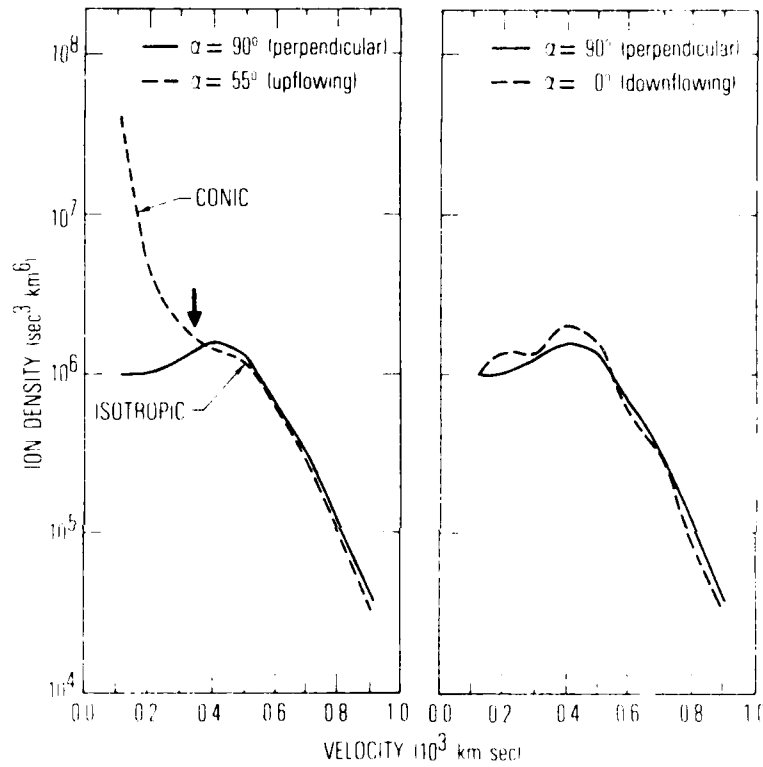


Fig. 2. Two plots of ion density as a function of velocity for the data shown in Figure 1. The left panel compares the upflowing ion conic spectrum with the perpendicular (90° pitch angle) spectrum. The right panel compares the downflowing (0° pitch angle) spectrum with the perpendicular spectrum.

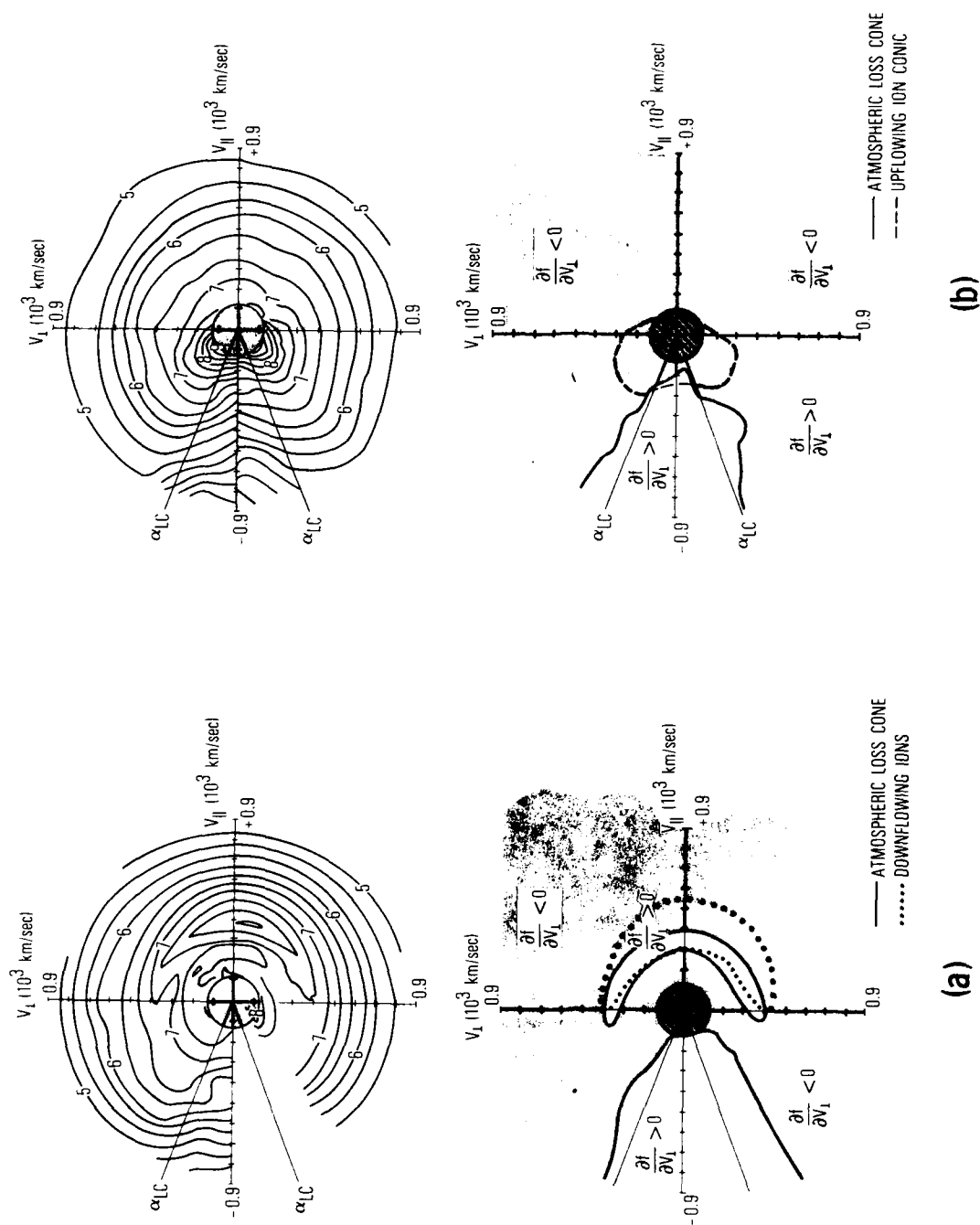


Fig. 3. Ion distributions from the S3-3 satellite at high latitude, near apogee on the dayside, showing (a) a downflowing ion distribution with a peak near 400 km/sec, and (b) an ion conic distribution with no downflowing ion beam.

similar to Figure 1. Indeed the regions of velocity that contribute to positive perpendicular velocity gradients are almost identical to those in Figure 1, even though there is no evidence of an ion conic in this case. On the other hand, the ion conic example in Figure 3b has no downflowing beam, and the only region that contributes a positive perpendicular velocity gradient is the high-energy loss cone. Again, the key element in the formation of a ring distribution is the downflowing ion population, not the upflowing ion conic.

III. CONCLUSIONS

Auroral ion distributions possess a number of features that might lead to plasma wave instabilities. The stability of upflowing accelerated ion beams has already been treated in some detail. Perhaps the downflowing ion beams presented in this report might also be subject to similar beam instabilities. The downflowing ion beams, under the influence of the defocussing magnetic mirror force, also form rings of energetic ions, which have regions of positive perpendicular velocity gradients, making them potentially unstable to flute mode instabilities. Upflowing ion conics, on the other hand, neither have peaked energy spectra nor are well represented by ion ring models.

REFERENCES

- Burch, J. L., P. H. Reiff, R. A. Heelis, J. D. Winningham, W. B. Hanson, C. Gurgiolo, J. D. Menietti, R. A. Hoffman, and J. N. Barfield, Plasma injection and transport in the mid-altitude polar cusp, Geophys. Res. Lett. 9, 921 (1982).
- Cattell, C., and M. Hudson, Flute mode waves near ω_{UH} excited by ion rings in velocity space, Geophys. Res. Lett. 9, 1167 (1982).
- Chang, T., and B. Coppi, Lower hybrid acceleration and ion evolution in the supraauroral region, Geophys. Res. Lett. 8, 1253 (1981).
- Dusenbery, P. B., and L. R. Lyons, Generation of ion conic distributions by downward auroral currents, J. Geophys. Res. 86, 7627 (1981).
- Fennell, J. F., P. F. Mizera, and D. R. Croley, Jr., Observations of ion and electron distributions during the July 29 and July 30, 1977 storm period, Proceedings of Magnetospheric Boundary Layers Conference, Alpbach, Austria, 11-15 June 1979.
- Ghielmetti, A. G., R. G. Johnson, R. D. Sharp, and E. G. Shelley, The latitudinal, diurnal, and altitudinal distributions of upward flowing energetic ions of ionospheric origin, Geophys. Res. Lett. 5, 59 (1978).
- Ghielmetti, A. G., R. D. Sharp, E. G. Shelley, and R. G. Johnson, Downward flowing ions and evidence for injection of ionospheric ions into the plasma sheet, J. Geophys. Res. 84, 5781 (1979).
- Gorney, D. J., A. Clarke, D. Croley, J. Fennell, J. Luhmann, and P. Mizera, The distribution of ion beams and conics below 8000 km, J. Geophys. Res. 86, 83 (1981).
- Greenspan, M. E., and E. C. Whipple, Jr., Energization of ions by oblique double layers, submitted to J. Geophys. Res. (1982).
- Kaufman, R. L., and P. M. Kintner, The stability of upgoing ion beams, submitted to J. Geophys. Res. (1982).
- Kintner, P. M., On the distinction between electrostatic ion cyclotron waves and ion cyclotron harmonic waves, Geophys. Res. Lett. 7, 585 (1980).
- Kintner, P. M., and D. J. Gorney, A search for the transverse acceleration process which is the source of ion conics, submitted to J. Geophys. Res. 89, 937 (1982).

- Klumpar, D. M., Transversely accelerated ions above the auroral ionosphere, Proceedings of the 23rd Annual Meeting of the Division of Plasma Physics, 12-16 October, New York (1981).
- Klumpar, D. M., Transversely accelerated ions: An ionospheric source of hot magnetospheric ions, J. Geophys. Res. 84, 4229 (1979).
- Lennartsson, W., On the consequences of the interaction between the auroral plasma and the geomagnetic field, Planet. Space Sci. 28, 135 (1980).
- Lysak, R. L., M. K. Hudson, and M. Temerin, Ion heating by strong ion cyclotron turbulence, J. Geophys. Res. 85, 678 (1980).
- Okuda, H., and M. Ashour-Abdalla, Formation of a conical distribution and intense ion heating in the presence of hydrogen cyclotron waves, Geophys. Res. Lett. 8, 811 (1981).
- Reiff, P. H., T. W. Hill, and J. L. Burch, Solar wind plasma injection at the dayside magnetospheric cusp, J. Geophys. Res. 82, 479 (1977).
- Roth, I., and M. K. Hudson, Particle simulations of electrostatic emissions near the lower hybrid frequency, submitted to J. Geophys. Res. (1982).
- Sharp, R. D., R. G. Johnson, and E. G. Shelley, Observation of an ionospheric acceleration mechanism producing energetic (keV) ions primarily normal to the geomagnetic field direction, J. Geophys. Res. 82 3324 (1977).
- Shelley, E. G., R. D. Sharp, and R. G. Johnson, Satellite observations of an ionospheric acceleration mechanism, Geophys. Res. Lett. 3, 654 (1976a).
- Shelley, E. G., R. D. Sharp, and R. G. Johnson, He^{++} and H^+ flux measurements in the dayside cusp: estimates of convection electric field, J. Geophys. Res. 81, 2363 (1976b).
- Ungstrup, E., D. M. Klumpar, and W. J. Heikkila, Heating of ions to super-thermal energies in the topside ionosphere by electrostatic ion cyclotron waves, J. Geophys. Res. 84, 509 (1979).

LABORATORY OPERATIONS

The Laboratory Operations of The Aerospace Corporation is conducting experimental and theoretical investigations necessary for the evaluation and application of scientific advances to new military space systems. Versatility and flexibility have been developed to a high degree by the laboratory personnel in dealing with the many problems encountered in the nation's rapidly developing space systems. Expertise in the latest scientific developments is vital to the accomplishment of tasks related to these problems. The laboratories that contribute to this research are:

Aerophysics Laboratory: Launch vehicle and reentry fluid mechanics, heat transfer and flight dynamics; chemical and electric propulsion, propellant chemistry, environmental hazards, trace detection; spacecraft structural mechanics, contamination, thermal and structural control; high temperature thermomechanics, gas kinetics and radiation; cw and pulsed laser development including chemical kinetics, spectroscopy, optical resonators, beam control, atmospheric propagation, laser effects and countermeasures.

Chemistry and Physics Laboratory: Atmospheric chemical reactions, atmospheric optics, light scattering, state-specific chemical reactions and radiation transport in rocket plumes, applied laser spectroscopy, laser chemistry, laser optoelectronics, solar cell physics, battery electrochemistry, space vacuum and radiation effects on materials, lubrication and surface phenomena, thermionic emission, photosensitive materials and detectors, atomic frequency standards, and environmental chemistry.

Computer Science Laboratory: Program verification, program translation, performance-sensitive system design, distributed architectures for spaceborne computers, fault-tolerant computer systems, artificial intelligence and microelectronics applications.

Electronics Research Laboratory: Microelectronics, GaAs low noise and power devices, semiconductor lasers, electromagnetic and optical propagation phenomena, quantum electronics, laser communications, lidar, and electro-optics; communication sciences, applied electronics, semiconductor crystal and device physics, radiometric imaging; millimeter wave, microwave technology, and RF systems research.

Materials Sciences Laboratory: Development of new materials: metal matrix composites, polymers, and new forms of carbon; nondestructive evaluation, component failure analysis and reliability; fracture mechanics and stress corrosion; analysis and evaluation of materials at cryogenic and elevated temperatures as well as in space and enemy-induced environments.

Space Sciences Laboratory: Magnetospheric, auroral and cosmic ray physics, wave-particle interactions, magnetospheric plasma waves; atmospheric and ionospheric physics, density and composition of the upper atmosphere, remote sensing using atmospheric radiation; solar physics, infrared astronomy, infrared signature analysis; effects of solar activity, magnetic storms and nuclear explosions on the earth's atmosphere, ionosphere and magnetosphere; effects of electromagnetic and particulate radiations on space systems; space instrumentation.

END

FILMED

9-85

DTIC